

Since the system is under constant illumination and in thermal equilibrium, all the population numbers are time independent and are equal to the Boltzmann distribution numbers. Insertion of the expression for  $n_i$  from (A2) into (A5) and simplification produces the expression

$$\phi = \frac{\sum_{i=1}^p k_{ir} e^{-\epsilon_i/kT}}{\sum_{j=1}^p k_j e^{-\epsilon_j/kT}}$$

This equation is easily transformed into the final expression

$$\phi = \frac{\sum_{i=1}^p k_{ir} e^{-\Delta\epsilon_{i-1}/kT}}{\sum_{j=1}^p k_j e^{-\Delta\epsilon_{j-1}/kT}} \quad (\text{A6})$$

which becomes eq 2 in the text upon being particularized to a three-level manifold with a twofold degenerate second level.

We define  $I_i$ , the fraction of radiation originating at level  $i$  of the emitting manifold as the ratio of the rate of radiative decay from level  $i$  to the rate of radiative decay from all levels.

$$I_i = n_i k_{ir} / \sum_i n_i k_{ir}$$

Once again the insertion of Boltzmann distribution numbers and simplification of the result produces the desired expression

$$I_i = k_{ir} e^{-\Delta\epsilon_{i-1}/kT} / \sum_j k_j e^{-\Delta\epsilon_{j-1}/kT} \quad (\text{A7})$$

This equation, adapted to the appropriate level scheme, was used to generate the plots of Figure 8.

## References and Notes

- (1) Research supported by AFOSR(NC)-OAR, USAF Grant AFOSR-72-2207.
- (2) Abstracted from a dissertation by G. D. Hager submitted to the Graduate School of Washington State University in partial fulfillment of the requirements for the degree Doctor of Philosophy, 1973.
- (3) NDEA Fellow, 1968-1971.
- (4) R. W. Harrigan and G. A. Crosby, *J. Chem. Phys.*, **59**, 3468 (1973); R. W. Harrigan, G. D. Hager, and G. A. Crosby, *Chem. Phys. Lett.*, **21**, 487 (1973).
- (5) G. D. Hager, R. J. Watts, and G. A. Crosby, *J. Am. Chem. Soc.*, **97**, 7037 (1975).
- (6) K. W. Hipps and G. A. Crosby, *J. Am. Chem. Soc.*, **97**, 7042 (1975).
- (7) R. J. Watts and G. A. Crosby, *J. Am. Chem. Soc.*, **93**, 3184 (1971).
- (8) D. H. W. Carstens and G. A. Crosby, *J. Mol. Spectrosc.*, **34**, 113 (1970).
- (9) D. M. Klassen and G. A. Crosby, *J. Chem. Phys.*, **48**, 1853 (1968).
- (10) J. N. Demas and G. A. Crosby, *J. Am. Chem. Soc.*, **93**, 2841 (1971).
- (11) R. J. Watts and G. A. Crosby, *J. Am. Chem. Soc.*, **94**, 2606 (1972).
- (12) R. J. Watts, unpublished results, this laboratory.
- (13) R. W. Harrigan and G. A. Crosby, *Spectrochim. Acta. Part A*, **26**, 2225 (1970).
- (14) "RCA Photomultiplier Tubes," Technical Publication PIT-700B, Radio Corp. of America, Dec 1971, pp 56-57.
- (15) G. A. Crosby, R. J. Watts, and D. H. W. Carstens, *Science*, **170**, 1195 (1970).
- (16) T. Azumi, C. M. O'Donnell, and S. P. McGlynn, *J. Chem. Phys.*, **45**, 2735 (1966).
- (17) J. S. Griffith, "The Theory of Transition-Metal Ions", Cambridge University Press, Cambridge, England, 1971.
- (18) L. E. Orgel, *J. Chem. Soc.*, 3683 (1961).
- (19) M. J. D. Powell, *Comput. J.*, **7**, 303 (1965).
- (20) D. C. Baker and G. A. Crosby, *Chem. Phys.*, **4**, 428 (1974).
- (21) M. A. El-Sayed, *Acc. Chem. Res.*, **4**, 23 (1971).
- (22) R. J. Watts and G. A. Crosby, unpublished results, this laboratory.
- (23) B. J. Pankuch and G. A. Crosby, unpublished results, this laboratory.
- (24) D. E. Lacky and G. A. Crosby, unpublished results, this laboratory.
- (25) G. A. Crosby, G. D. Hager, K. W. Hipps, and M. L. Stone, *Chem. Phys. Lett.*, **28**, 497 (1974).
- (26) K. W. Hipps and G. A. Crosby, *Inorg. Chem.*, **13**, 1543 (1974).

## Charge-Transfer Excited States of Ruthenium(II) Complexes. II. Relationship of Level Parameters to Molecular Structure<sup>1,2</sup>

G. D. Hager,<sup>3</sup> R. J. Watts, and G. A. Crosby\*

Contribution from the Department of Chemistry, Washington State University, Pullman, Washington 99163. Received November 19, 1974

**Abstract.** Energy-level splittings and radiative and radiationless rate constants for the lowest excited  $d\pi^*$  states of seven ruthenium(II) cations are compared and related to molecular structure. Exchange integrals between the promoted electron on the ligand system and the remaining core electrons have been calculated to lie in the range of 18-65  $\text{cm}^{-1}$ , indicative of essential removal of the electron from the core during the excitation. Relationships between radiative and radiationless rate constants for individual levels have been demonstrated, and a dominant role for spin-orbit coupling in determining the energy-level splittings and promoting rapid relaxation among excited states has been assumed. Relations between excited state properties and chemical and electrochemical behavior are discussed.

Quantitative spectroscopic studies of the metal-to-ligand charge-transfer (CTTL) excited states of ruthenium(II) with bipyridine and substituted-bipyridine ligands have been reported in the preceding paper of this series.<sup>4</sup> The data strongly supported the previously proposed orbital and symmetry assignments of the lowest excited levels that are responsible for the observed photoluminescence.<sup>5</sup> In this article we present the results of extensive investigations of the properties of the lowest excited electronic states of ruthenium(II) complexes containing 1,10-phenanthroline and substituted 1,10-phenanthroline as ligands. The spectroscopic properties of these molecules not only corroborate the conclusions reached in the previous paper but, in conjunction with the other data, allow the detailed properties of the ex-

cited states of both series to be correlated with molecular structure.

### Experimental Section

**Synthesis and Sample Preparation.** The tris(1,10-phenanthroline)ruthenium(II) iodide monohydrate,  $[\text{Ru}(\text{phen})_3]\text{I}_3$ , was a sample prepared by Klassen.<sup>6</sup> Tris(4,7-diphenyl-1,10-phenanthroline)ruthenium(II) chloride pentahydrate,  $[\text{Ru}(4,7\text{-Ph}_2\text{phen})_3]\text{Cl}_2$ , was prepared previously.<sup>7</sup> Both the tris(4,7-dimethyl-1,10-phenanthroline)ruthenium(II) chloride septahydrate,  $[\text{Ru}(4,7\text{-Me}_2\text{phen})_3]\text{Cl}_2$ , and the tris(5,6-dimethyl-1,10-phenanthroline)ruthenium(II) chloride nonahydrate,  $[\text{Ru}(5,6\text{-Me}_2\text{phen})_3]\text{Cl}_2$ , were prepared and purified by published methods for analogous compounds.<sup>7</sup>

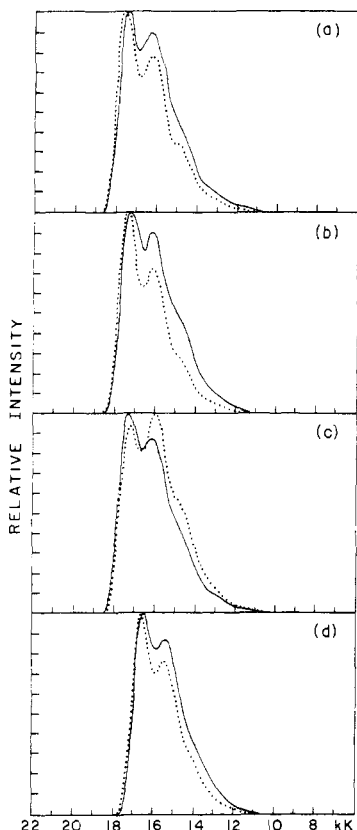


**Figure 1.** Luminescence spectra of ruthenium(II) complexes in PMM: (a)  $[\text{Ru}(\text{phen})_3]\text{Cl}_2$ , (b)  $[\text{Ru}(5,6\text{-Me}_2\text{phen})_3]\text{Cl}_2$ , (c)  $[\text{Ru}(4,7\text{-Me}_2\text{phen})_3]\text{Cl}_2$ , (d)  $[\text{Ru}(4,7\text{-Ph}_2\text{phen})_3]\text{Cl}_2$ ; (—) 4.2 K, (···) 77 K.

Anal. Calcd for  $[\text{Ru}(\text{C}_{14}\text{H}_{12}\text{N}_2)_3]\text{Cl}_2 \cdot 7\text{H}_2\text{O}$ : C, 55.14; H, 4.62; Cl, 7.75; N, 9.18. Found: C, 54.67; H, 4.56; Cl, 9.14; N, 9.48. Calcd for  $[\text{Ru}(\text{C}_{14}\text{H}_{12}\text{N}_2)_3]\text{Cl}_2 \cdot 9\text{H}_2\text{O}$ : C, 53.05; H, 4.87; Cl, 7.45; N, 8.83. Found: C, 53.46; H, 4.28; Cl, 7.34; N, 8.99.

For spectral and luminescence quantum yield measurements the substances were dissolved in ethanol-methanol (4:1, v/v). For the temperature-dependence studies the samples were incorporated into polymethylmethacrylate (PMM) matrices as described in part I of this series.<sup>4</sup>

**Measurements.** All absorption and photoluminescence spectra were recorded using procedures identical with those employed for the analogous bipyridine complexes.<sup>4</sup> Quantum yields, decay times, and relative intensities were also measured in the same manner as described previously. Because of the close similarities of the optical properties of the phenanthroline and bipyridine complexes even the same filtering systems could be employed for both sets of molecules. The samples were all well behaved and suffered no measurable deterioration even under prolonged exposure to intense uv radiation.

### Results of Spectroscopic Measurements

Both the absorption spectrum (82 K) and the emission spectrum (77 K) of  $[\text{Ru}(\text{phen})_3]\text{I}_2$  in a glass have been published.<sup>6</sup> For its quantum yield we adopt the value of 0.58 that was determined previously in an ethanol-methanol glass (4:1, v/v) at 77 K.<sup>8</sup> The absorption and luminescence spectra of  $[\text{Ru}(4,7\text{-Ph}_2\text{phen})_3]\text{Cl}_2$  have been reported,<sup>7</sup> and a quantum yield of 0.68 has been measured in the same glass at 77 K.<sup>9</sup> Quantum yields of  $0.65 \pm 0.03$  for  $[\text{Ru}(4,7\text{-Me}_2\text{phen})_3]\text{Cl}_2$  and  $0.57 \pm 0.03$  for  $[\text{Ru}(5,6\text{-Me}_2\text{phen})_3]\text{Cl}_2$  were obtained in ethanol-methanol glasses (4:1, v/v) at 77 K. All yields were assumed to be essentially matrix independent and thus valid for the systems when dissolved in the PMM matrix. The uncertainties introduced by this procedure are discussed in part I.

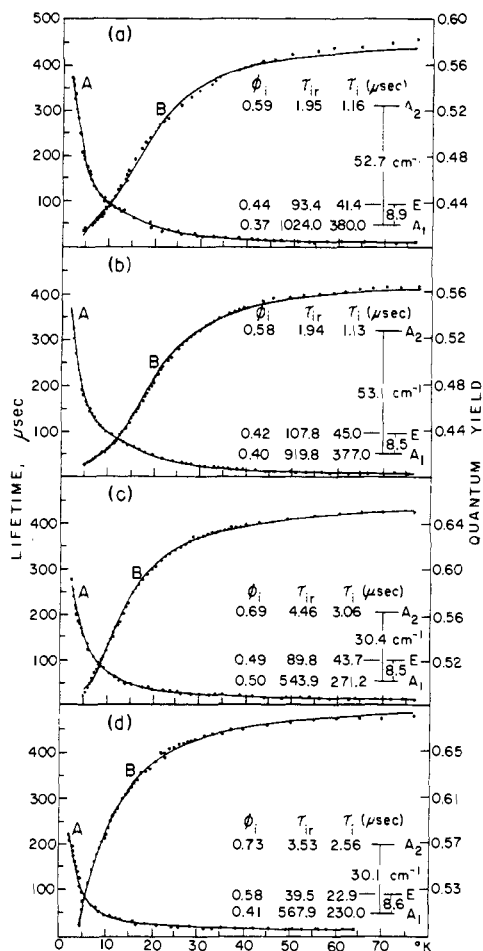


**Figure 2.** Temperature dependence of the lifetimes and quantum yields of ruthenium(II) complexes and computer generated parameters for each luminescing charge-transfer manifold: (a)  $[\text{Ru}(\text{phen})_3]\text{Cl}_2$  in PMM, (b)  $[\text{Ru}(5,6\text{-Me}_2\text{phen})_3]\text{Cl}_2$  in PMM, (c)  $[\text{Ru}(4,7\text{-Me}_2\text{phen})_3]\text{Cl}_2$  in PMM, (d)  $[\text{Ru}(4,7\text{-Ph}_2\text{phen})_3]\text{Cl}_2$  in PMM; (···) experimental values, (—) "best fit" computer generated curves. Lifetimes, curve A, are read from the left ordinate; quantum yields, curve B, from the right.

The luminescence spectra of the four complexes at 4.2 and 77 K in the PMM matrix are shown in Figure 1. The similarity of this set of spectra with the set obtained from the bipyridine complexes is striking.<sup>4</sup> Not only does the luminescence fall in the same spectral region but the band contours are also very similar. As the temperature is lowered, the second vibrational peak grows in at the expense of the highest energy one except for  $[\text{Ru}(4,7\text{-Me}_2\text{phen})_3]\text{Cl}_2$ . In contrast to the other six, the temperature dependence of the spectrum for this complex is curiously reversed; the second peak loses intensity as the temperature is lowered.

In Figure 2 both the lifetime and quantum yield of each complex are displayed as a function of temperature between 1.8 and 77 K. The general pattern of behavior found for the three bipyridine species is faithfully repeated by the set of four phenanthrolines. As the temperature is lowered, the total photoluminescence quantum yield steadily decreases while the observed decay time monotonically increases.

### Excited State Parameters

To obtain energy-level splittings and decay parameters for the electronic excited states giving rise to the photoluminescence, we employed the procedures described in part I.<sup>4</sup> A phenomenological model consisting of three levels that remain in Boltzmann equilibrium during the time that the ensemble decays to the ground state was assumed. The

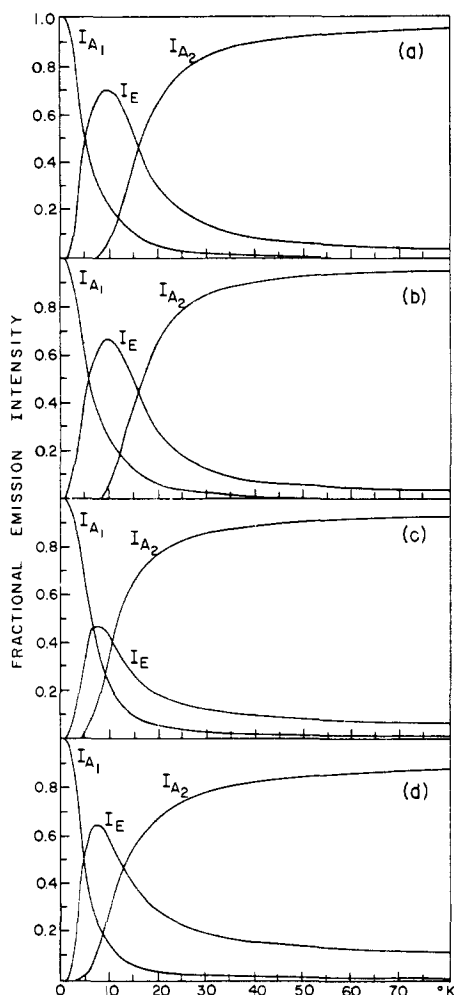


Figure 3. Temperature dependence of the fractional intensity of light emanating from the  $A_1$ , E, and  $A_2$  states of (a)  $[\text{Ru}(\text{phen})_3]\text{Cl}_2$ . (b)  $[\text{Ru}(5,6\text{-Me}_2\text{phen})_3]\text{Cl}_2$ . (c)  $[\text{Ru}(4,7\text{-Me}_2\text{phen})_3]\text{Cl}_2$ . (d)  $[\text{Ru}(4,7\text{-Ph}_2\text{phen})_3]\text{Cl}_2$  in PMM.

reader is referred to part I for a detailed description of the model and the assumptions underlying it. The level scheme is depicted in Figure 7 of part I.

Computer analyses of the temperature-dependent lifetime and quantum yield curves of Figure 2 produced the requisite splittings and rate constants for the emitting manifold. Equations 1 and 2 of part I were employed. Also included in Figure 2 are the characteristics of the excited manifold responsible for the observed phenomena as obtained from the computer. Similarities with the level sets found for the analogous bipyridine species are obvious, but we defer detailed discussion of them until later. We remark, however, that the *radiative* rate constants for these molecules corroborate the symmetry assignments made previously on the basis of total rate constants.<sup>5</sup> These symmetry labels are also included in the figure. Thus, as for the bipyridine complex ions, the empirical evidence from the four phenanthroline complex ions of ruthenium(II) strongly supports the concept of a closely packed manifold of three levels being responsible for the luminescence and arising from a  $d\pi^*(a_2)$  excited configuration.

Utilizing the equations derived in the appendix of part I we can also calculate fractional intensity distributions for each system as a function of temperature. These plots are given in Figure 3. One sees that the curves are qualitatively the same as those presented for the bipyridine complexes in paper I. Because the energy-level splittings of the phenan-

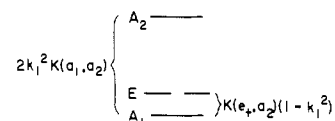


Figure 4. Splittings of the lowest  $d\pi^*$  manifold in terms of theoretical coupling parameters.

throline complexes are smaller than those found for the other series, the prospects for weighting the observed luminescence toward a particular level by specification of temperature are less favorable. This statement holds particularly for the E level. In the worst case,  $[\text{Ru}(4,7\text{-Me}_2\text{phen})_3]\text{Cl}_2$ , the analysis predicts that, even at the optimum temperature ( $\sim 8$  K), only 46% of the emitted light originates from the E states. Thus, more than half the total light output at 8 K arises from the other two levels, vitiating the conclusions to be drawn from any polarization measurements designed to confirm the assignment. The data indicate that polarization experiments would be more fruitful when carried out on the bipyridine molecules rather than on phenanthroline species.

### Discussion

We turn now to a detailed analysis of the properties of the manifold of excited states inferred from the luminescence measurements. At the outset we assume that both the bipyridine and phenanthroline complexes can be treated within the same theoretical formalism and that they all possess  $D_3$  symmetry. We also adopt the description  $d\pi^*(a_2)$  for the lowest excited electronic configuration and accept the group theoretical assignments to be  $A_1$ , E, and  $A_2$  in order of increasing energy. Furthermore we adopt the quantitative description of the lowest cluster of excited states as developed in paper III of this series. Henceforth the discussion will focus on these levels within the context of the model.

As displayed in Figure 4 and derived in part III, the splittings of the lowest cluster of emitting levels are dependent on both electrostatic and spin-orbit interactions. In principle, all three parameters are measurable. The parameter  $k_1^2$  appears in the definition of the eigenfunction for the ground state of the  $d^5$  core (see part III). Its value can be estimated from spin resonance measurements on the species obtained by oxidizing the ruthenium(II) complex ion to the ruthenium(III) species. Two exchange integrals appear:  $K(e_+, a_2)$  is the nonclassical electrostatic interaction between the promoted electron residing in the  $\pi(a_2)$  orbital on the ligand system and an electron in the core populating a d orbital of e symmetry;  $K(a_1, a_2)$  is the exchange interaction between the promoted electron and one occupying the d orbital extending along the principal symmetry axis of the complex.

**Evaluation of Exchange Interactions.** Figure 5 displays the energy-level diagrams for the seven systems analyzed. Two features are manifest. The energy gaps for the three bipyridine complexes are larger than those of the phenanthroline series, and substitution in the 4,7 positions of the phenanthroline moieties causes a further drastic reduction in the  $A_1$ - $A_2$  gap. These features can be quantified. As discussed in part III, spin-resonance measurements on  $[\text{Ru}(\text{bpy})_3]^{3+}$  and  $[\text{Ru}(\text{phen})_3]^{3+}$  lead to a value of 0.83 and 0.86, respectively, for  $k_1^2$ . If we adopt a compromise value of 0.85 for  $k_1^2$  for all the molecules, we can then evaluate  $K(a_1, a_2)$  and  $K(e_+, a_2)$  from the experimental splittings. The results of these calculations are given in Table I.

We note in Table I that the reduced splittings apparent in the phenanthroline series are reflected in smaller values of the exchange integrals. This points toward a higher degree

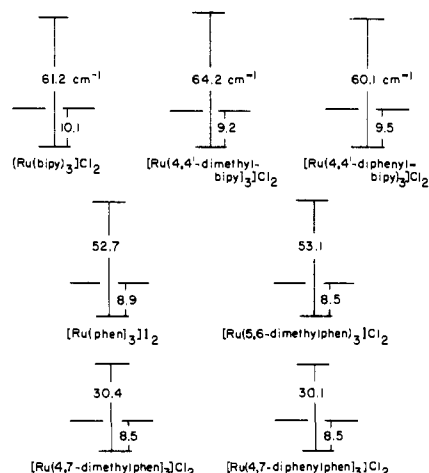


Figure 5. Composite energy-level diagram for trigonal ruthenium(II) complexes.

Table I. Experimental Exchange Integrals for the  $d\pi^*(a_2)$  Excited Configuration

| Compound  | $K(a_1, a_2)^a$<br>( $\text{cm}^{-1}$ ) | $K(e+, a_2)$<br>( $\text{cm}^{-1}$ ) | $K(a_1, a_2)/$<br>$K(e+, a_2)$ |
|---|---|--------------------------------------|--------------------------------|
| [Ru(bpy) <sub>3</sub> ]Cl <sub>2</sub>                      | 36                                      | 63                                   | 0.57                           |
| [Ru(4,4'-Me <sub>2</sub> bpy) <sub>3</sub> ]Cl <sub>2</sub> | 38                                      | 57                                   | 0.66                           |
| [Ru(4,4'-Ph <sub>2</sub> bpy) <sub>3</sub> ]Cl <sub>2</sub> | 36                                      | 59                                   | 0.61                           |
| [Ru(phen) <sub>3</sub> ]I <sub>2</sub>                      | 31                                      | 56                                   | 0.55                           |
| [Ru(5,6-Me <sub>2</sub> phen) <sub>3</sub> ]Cl <sub>2</sub> | 32                                      | 53                                   | 0.60                           |
| [Ru(4,7-Me <sub>2</sub> phen) <sub>3</sub> ]Cl <sub>2</sub> | 18                                      | 53                                   | 0.33                           |
| [Ru(4,7-Ph <sub>2</sub> phen) <sub>3</sub> ]Cl <sub>2</sub> | 18                                      | 53                                   | 0.33                           |

<sup>a</sup> Exchange integrals calculated with  $k_1^2 = 0.84$  (see Figure 4).

of delocalization of the promoted electron over the ligand system in the phenanthroline complexes than in the bipyridine ones, a result in accord with the greater extent of the  $\pi$ -structure of *o*-phenanthroline. The ratio  $K(a_1, a_2)/K(e, a_2)$  also appears intuitively reasonable. The *e* orbitals of the core extend out into the plane of the ligands containing the promoted electron, whereas the  $a_1$  is localized along the axis perpendicular to the twofold axes bisecting the ligands.

The exceptional cases are the two complex ions containing substituents in the 4 and 7 positions of the three phenanthroline ligands. The small  $A_1$ - $A_2$  splittings are reflected in the low values for  $K(a_1, a_2)$  and the unusually low ratio of the two exchange integrals. If we seek the cause for the anomalously low values of  $K(a_1, a_2)$  for the 4,7-substituted compounds in the shape of the  $\pi^*(a_2)$  orbital, we see that these positions are indeed heavily represented in this orbital. A glance at Figure 4 of ref 10, which shows the lowest antibonding orbital, confirms that 4,7 substitution should affect the exchange integrals, whereas 5,6 substitution should cause little effect, a conclusion borne out by our experiments. It is, however, difficult to rationalize all the large changes in  $K(a_1, a_2)$  by electrostatic arguments. If we assert that the sensitivity to 4,7 substitution can be laid to the properties of the  $\pi^*(a_2)$ -antibonding orbital, the distribution of the lowest vacant molecular orbital also indicates that 4,4' substitution on the bipyridine complexes should produce a similar result. No such effect is observed.

An obvious alternative explanation of the small splittings observed for the 4,7-substituted complexes is that the source lies in the value of  $k_1^2$ . Since the only reported measurements were made on the two parent complexes, we assumed a compromise value of 0.84 for  $k_1^2$  to obtain Table I. If we allow  $k_1^2$  and both exchange integrals to vary, then the system is overdetermined, and no entirely satisfactory set of values for these parameters can be extracted from the

Table II. Experimental Parameters for the Lowest  $d\pi^*(a_2)$  CTTL Excited States of Ruthenium(II) Complexes

| Compound  | Symmetry       | $\tau_i$<br>( $\mu\text{sec}$ ) | $\tau_{ir}$<br>( $\mu\text{sec}$ ) | $\tau_{iq}$<br>( $\mu\text{sec}$ ) | $\phi_i$ |
|---|----------------|---------------------------------|------------------------------------|------------------------------------|----------|
| [Ru(bpy) <sub>3</sub> ]Cl <sub>2</sub>                      | A <sub>2</sub> | 0.683                           | 1.69                               | 0.98                               | 0.404    |
|   | E              | 18.8                            | 81.7                               | 24.4                               | 0.230    |
|   | A <sub>1</sub> | 183.1                           | 1091.5                             | 206.4                              | 0.167    |
| [Ru(4,4'-Me <sub>2</sub> bpy) <sub>3</sub> ]Cl <sub>2</sub> | A <sub>2</sub> | 0.58                            | 1.59                               | 0.91                               | 0.364    |
|   | E              | 18.8                            | 94.5                               | 23.3                               | 0.198    |
|   | A <sub>1</sub> | 152.0                           | 1142.5                             | 175.3                              | 0.133    |
| [Ru(4,4'-Ph <sub>2</sub> bpy) <sub>3</sub> ]Cl <sub>2</sub> | A <sub>2</sub> | 0.69                            | 1.19                               | 1.75                               | 0.597    |
|   | E              | 17.6                            | 43.1                               | 34.1                               | 0.407    |
|   | A <sub>1</sub> | 164.8                           | 518.6                              | 240.7                              | 0.317    |
| [Ru(phen) <sub>3</sub> ]I <sub>2</sub>                      | A <sub>2</sub> | 1.16                            | 1.95                               | 2.85                               | 0.594    |
|   | E              | 41.4                            | 93.4                               | 74.3                               | 0.443    |
|   | A <sub>1</sub> | 380.0                           | 1024.0                             | 612.8                              | 0.371    |
| [Ru(5,6-Me <sub>2</sub> phen) <sub>3</sub> ]Cl <sub>2</sub> | A <sub>2</sub> | 1.13                            | 1.94                               | 2.70                               | 0.582    |
|   | E              | 45.0                            | 107.8                              | 77.1                               | 0.417    |
|   | A <sub>1</sub> | 377.0                           | 919.8                              | 636.6                              | 0.409    |
| [Ru(4,7-Me <sub>2</sub> phen) <sub>3</sub> ]Cl <sub>2</sub> | A <sub>2</sub> | 3.06                            | 4.46                               | 9.47                               | 0.686    |
|   | E              | 43.7                            | 89.8                               | 84.9                               | 0.486    |
|   | A <sub>1</sub> | 271.2                           | 544.0                              | 539.6                              | 0.498    |
| [Ru(4,7-Ph <sub>2</sub> phen) <sub>3</sub> ]Cl <sub>2</sub> | A <sub>2</sub> | 2.56                            | 3.53                               | 9.31                               | 0.725    |
|   | E              | 22.9                            | 39.5                               | 54.1                               | 0.578    |
|   | A <sub>1</sub> | 230.0                           | 567.9                              | 386.6                              | 0.405    |

data. The small splittings strongly indicate, however, that 4,7 substitution lowers  $k_1^2$  considerably and also reduces both exchange integrals. EPR data on the oxidized substituted species would shed light on this problem. A third alternative is that the model is too simple to account for nuances in the splittings due to substitution.

**Rate Constants.** All the experimental parameters drawn from the data that relate to the properties of the individual levels are assembled in Table II. Before generalizing from these quantities, it is pertinent to make a few statements about the degrees of precision and accuracy that can be attributed to these values. As discussed previously,<sup>5</sup> we have been able to devise no technique for assigning meaningful error bars to the energy-level or rate-constant values. The parameters are extracted from a curve-fitting technique that weights each experimental value of quantum yield and lifetime equally. Statistical jitter in these data points is reflected in the parameters, but in an, as yet, unknown way. We also have the real problem of assessing the accuracy of the quantum yields. As discussed elsewhere,<sup>11,12</sup> the measured yields could certainly have a systematic error of 10% incorporated in them. This would be reflected in the values of  $\tau_{ir}$ ,  $\tau_{iq}$ , and  $\phi$  listed in the table, as would any dependence of the quantum yield on matrix (see part I). Given these uncertainties we have listed the values in Table II as they were obtained from the computer. The number of significant figures is certainly less than indicated. We believe, however, that the *relative magnitudes* of the listed values are meaningful and that significant physical information bearing on the electronic structures of the complexes is contained in them. This is the view we adopt in what follows.

Perusal of Table II shows that the similarities between the energy-level schemes for bipyridine and phenanthroline complexes are reflected in the mean lives of the excited states. The lowest ( $A_1$ ) level is long-lived, the second (*E*) level is an order of magnitude shorter lived, and the uppermost ( $A_2$ ) level has a substantially shorter life yet. This generalization holds for both the radiative ( $\tau_{ir}$ ) and radiationless ( $\tau_{iq}$ ) lives of the states as well. The same trend is seen in the experimental quantum yields determined for each level. The  $A_1$  level has the smallest luminescence yield, the *E* level, an intermediate value, and the  $A_2$  level achieves the highest yield of all. The single exception is [Ru(4,7-Me<sub>2</sub>phen)<sub>3</sub>]Cl<sub>2</sub> for which the order of the first two yields is

reversed. Indeed, methyl substitution in either the 4,7 or 5,6 positions produces a near coincidence of the yields for the  $A_1$  and E levels.

When one searches for differences between the two sets of complexes, it becomes apparent that the phenanthrolines are, as a group, less susceptible to quenching than the bipyridines. Substituents produce changes in the quenching lives of the states, but they are less effective than a switch from bipyridine to phenanthroline ligands. The enhanced rigidity of the latter framework is reflected in all the levels of the lowest manifold, regardless of their symmetries. Radiative lives of the levels are evidently less dependent upon the details of the molecular framework of the ligand system than upon the nature and positions of substituents. Attaching a methyl group in the 4,4' positions of the bipyridines has no significant effect on any of the rate constants, but placing phenyl groups in these positions increases the radiative rate constants of all the levels while at the same time decreasing the radiationless ones. The capacity of phenyl substituents to improve quantum efficiencies of both ruthenium(II) and iridium(III) complexes has been noted previously.<sup>9</sup>

The unusual sensitivity to substitution in the 4,7 positions of the phenanthroline ligands is apparent in Table II. Attaching methyl groups in the 5,6 positions produces negligible changes in the rate constants, but the incorporation of either a set of methyl groups or phenyl groups at the 4,7 sites produces a sizeable *decrease* in both the radiative and the quenching lives of the  $A_1$  level. Substituents in these positions also produce increases in both the radiative and radiationless lives of the  $A_2$  level. Thus the data show the electronic states to be sensitive in a nonuniform way both to the nature of the substituent and to its position on the ligand.

If one ignores the many differences among the rate constants discussed above and focuses on the similarities, it appears that the sets of radiative and radiationless rate constants for a given molecule are related. Indeed, for several of the levels the numerical values of radiative and radiationless rates are almost identical. We infer that the matrix elements responsible for the radiative properties of a level are related to those controlling the radiationless ones. In any perturbation treatment of the radiationless problem for states of this type, the correct zero-order functions would be strongly spin-orbit coupled ones. Utilization of a formalism employing an uncoupled basis, such as employed for hydrocarbons<sup>13</sup> would be quite inappropriate in our view.

**Relaxation Rates.** An underlying assumption of our treatment of the kinetic data for all the complexes is that relaxation among the lowest manifold of emitting levels is rapid in comparison with relaxation to the ground state. As discussed in part I, the experimental data justify *a posteriori* this postulate. Previously a lower limit of  $10^{10} \text{ sec}^{-1}$  was set for relaxation from *higher* excited states down to the lowest (emitting) manifold.<sup>8</sup> Since, in the present view, spin-orbit coupling plays a dominant role in dictating the natures of all the excited states, there is no reason to suppose that relaxation among the states of the lowest set of levels should be any slower than relaxation to the manifold. We expect the lower limit of  $10^{10} \text{ sec}^{-1}$  to apply to the former case also. Since the rate is  $10^4$  greater than the fastest rate measured for depopulating any level to the ground state, the observation of strictly exponential decays in all measurements is understandable.

**Excited State Geometry.** Visualizing the  $d\pi^*$  excitation process as formal incipient oxidation from Ru(II) to Ru(III) leads one to expect large differences in molecular geometry between the ground and the excited  $d\pi^*$  states. Yet, as seen in Figure 1, and also in Figure 5 of paper I, the observed luminescences are all Franck-Condon allowed, in-

dicative of small geometrical changes during deexcitation. Our view of the  $d\pi^*$  excited configuration as a coupling between a Ru(III) ( $d^5$ ) ion and an excited electron on the ligand system appears to be applicable, however, because complete oxidation produces little change in bond lengths even of the hexaammines.<sup>14</sup> The band shapes observed from these complexes are in stark contrast to those observed from complexes exhibiting dd emission. For the latter systems enormous geometrical changes occur during excitation, although there is no change in formal oxidation number.<sup>15,16</sup>

### Chemical Implications

The view of  $d\pi^*$  excited states adopted here attributes the gross splitting of groups of levels to spin-orbit interactions localized on the central core and relegates electrostatic exchange forces between the promoted electron and the core electrons to the role of determining the fine structure of each group. The latter splittings are small ( $<100 \text{ cm}^{-1}$ ); whereas the former are considerably larger ( $\sim 1000 \text{ cm}^{-1}$ ). This situation is just the opposite of that found for the electronic states of organic molecules and has important chemical consequences.

Since these molecules are luminescent in fluid solution, they have become important as donors in energy-transfer experiments. Although the acceptor systems in these studies may have well-defined spin states, the donor states do not. Indeed, at any reasonable temperatures,  $kT$  is greater than the splittings of the lowest manifold and the ensemble is rapidly relaxing among the lowest electronic states. The donor "state" is thus best described as a  $d\pi^*$  configuration of closely spaced  $A_1$ , E, and  $A_2$  states having no meaningful spin label. The question of spin labeling states in complexes has been discussed earlier.<sup>17</sup>

According to the model, infinite separation of the promoted electron from the core (ionization) would collapse the energy diagram of Figure 4 to a single fourfold degenerate level. Thus the small values of the observed separations of the final states of the  $d\pi^*(a_2)$  clusters indicate a large separation of the promoted electron from the core. In the excited  $d\pi^*$  configuration the systems should be powerful reducing agents, a condition that has already been exploited.<sup>18</sup> Our data indicate that the excited 4,7-substituted molecules would be the most powerful reducing agents of those thus far investigated.

Strong chemical evidence that the creation of the  $d\pi^*$  excited configuration in these ruthenium(II) complexes by the absorption of a photon is an incipient formal oxidation comes from both chemical and electrochemical experiments on the reduction of the corresponding ruthenium(III) species. Bard and coworkers<sup>19</sup> have shown that electrogenerated chemiluminescence (ecl) is obtainable from solutions of  $[\text{Ru}(\text{bpy})_3]^{2+}$ . The postulated mechanisms involve the reduction of  $[\text{Ru}(\text{bpy})_3]^{3+}$  by several routes leading to the formation of  $[\text{Ru}(\text{bpy})_3]^{2+}$  in the  $d\pi^*$  excited configuration and subsequently to light emission. The near coincidence of the frequency of light caused by ecl and that stimulated by light absorption leaves little doubt that the same excited species is involved in both processes. There are indications, however, that other processes, and species, are involved.<sup>19</sup>

Because the view of the  $d\pi^*$  excited configuration expressed here is subject to mathematical quantification, it may be possible to relate the chemical and spectroscopic properties of series of complexes with similar ligands but possessing different metal ions. We defer these considerations until the model has been fully developed in the third paper of this series.

### References and Notes

- (1) Research supported by AFOSR(NC)-OAR, USAF Grant AFOSR-72-2207.

- (2) Abstracted in part from a dissertation by G. D. Hager submitted to the Graduate School of Washington State University in partial fulfillment of the requirements for the degree Doctor of Philosophy, 1973.
- (3) NDEA Fellow, 1968–1971.
- (4) Part I. G. D. Hager and G. A. Crosby, *J. Am. Chem. Soc.*, **97**, 7037 (1975).
- (5) R. W. Harrigan and G. A. Crosby, *J. Chem. Phys.*, **59**, 3468 (1973).
- (6) D. M. Klassen and G. A. Crosby, *J. Chem. Phys.*, **48**, 1853 (1968).
- (7) R. J. Watts and G. A. Crosby, *J. Am. Chem. Soc.*, **93**, 3184 (1971).
- (8) J. N. Demas and G. A. Crosby, *J. Am. Chem. Soc.*, **93**, 2841 (1971).
- (9) R. J. Watts and G. A. Crosby, *J. Am. Chem. Soc.*, **94**, 2606 (1972).
- (10) I. Hanazaki and S. Nagakura, *Inorg. Chem.*, **8**, 648 (1969).
- (11) J. N. Demas and G. A. Crosby, *J. Phys. Chem.*, **75**, 991 (1971).
- (12) J. N. Demas and G. A. Crosby, *J. Am. Chem. Soc.*, **92**, 7262 (1970).
- (13) B. R. Henry and W. Siebrand, *J. Chem. Phys.*, **54**, 1072 (1971).
- (14) H. C. Stynes and J. A. Ibers, *Inorg. Chem.*, **10**, 2304 (1971).
- (15) K. W. Hipps and G. A. Crosby, *Inorg. Chem.*, **13**, 1543 (1974).
- (16) G. A. Crosby, G. D. Hager, K. W. Hipps, and M. L. Stone, *Chem. Phys. Lett.*, **28**, 497 (1974).
- (17) G. A. Crosby, K. W. Hipps, and W. H. Elfring, Jr., *J. Am. Chem. Soc.*, **96**, 629 (1974).
- (18) C. R. Bock, T. J. Meyer, and D. G. Whitten, Abstracts, 167th National Meeting of the American Chemical Society, Los Angeles, Calif., April 1974, INOR 99.
- (19) N. E. Tokel-Takvoryan, R. E. Hemingway, and A. J. Bard, *J. Am. Chem. Soc.*, **95**, 6582 (1973).

## Charge-Transfer Excited States of Ruthenium(II) Complexes. III. An Electron–Ion Coupling Model for $d\pi^*$ Configurations<sup>1</sup>

K. W. Hipps and G. A. Crosby\*

*Contribution from the Department of Chemistry, Washington State University, Pullman, Washington 99163. Received November 19, 1974*

**Abstract:** An electron–ion (parent) coupling model first proposed on experimental and group theoretical grounds (R. W. Harrigan and G. A. Crosby, *J. Chem. Phys.*, **59**, 3468 (1973)) for predicting the symmetries of  $d\pi^*$  excited states has been mathematically developed. An energy level scheme for the lowest  $d\pi^*(a_2)$  excited configuration of trigonal  $d^6$  complexes has been developed in terms of a limited number of molecular parameters to be evaluated experimentally. The model satisfactorily rationalizes the experimental data on excited states of ruthenium(II) complexes of 2,2'-bipyridine and 1,10-phenanthroline obtained previously from decay time and quantum yield measurements and predicts a semiquantitative relationship between the  $g$  factors of excited states of a  $d^6$  complex and the ground states of the corresponding  $d^5$  species obtained by chemical oxidation. The extension of the coupling model to complexes of other ions and to ions with different symmetries is also discussed.

Extensive optical measurements on a series of ruthenium(II) complexes containing  $\pi$ -conjugated ligands have been reported previously.<sup>2–5</sup> A variety of experimental techniques was used. The main thrust of the research was to elucidate the nature of the low-lying charge-transfer (CT) excited states responsible for the unusual photoluminescence exhibited by these materials. The extensive experimental evidence led to a multiple-state model for the origin of the emission. Indeed, a combination of spectroscopic, transient decay, quantum yield, and magnetic measurements has produced a well-defined picture of the emitting manifold, including splittings, radiative and radiationless rate constants, and group theoretic symmetry labels. In addition a coupling model has emerged that offers a new view of the nature of CT excited states and provides a conceptual scheme for rationalizing their observed properties and for attaching symmetry labels.

In this paper we pursue the development of the coupling model for CT excited states mathematically. Our purpose is to place the intuitive group theoretical model induced from the experiments on a firm mathematical foundation. We show that the proposed model is not only subject to quantification in a straightforward way but also that it provides a basis for relating the experimental data thus far obtained to fundamental molecular parameters. It possesses the merits of relative simplicity and predictive capability. The mathematical extension offers valuable insight into the nature of CT excited states and provides a scheme for exploiting periodic table relationships among transition metal complexes for spectroscopic purposes.

### Electron–Ion (Parent) Coupling Model for $d\pi^*$ Excited States

Following the discussion of Harrigan and Crosby<sup>6</sup> we visualize the low-lying charge-transfer excited configurations in these systems to be the result of the promotion of a  $d$  electron, initially localized on the metal ion, to a  $\pi^*$ -antibonding orbital delocalized over the ligand system. The states are viewed as arising from electrostatic coupling between the promoted (optical) electron and the  $(n - 1)$  electrons remaining on the ion core. The core electrons are pictured to be strongly coupled both electrostatically and magnetically to produce well-defined core states. The final CT excited states of the  $d^n$  system are then visualized as arising from weak electrostatic coupling between the promoted (optical) electron on the ligand system and the strongly coupled core electrons on the central ion. The mathematical scheme adopted is first to couple one-electron spin orbitals on the  $(n - 1)$  electron core and find eigenkets of the core Hamiltonian. Next, these core eigenkets are combined with the spin orbitals of the promoted electron to generate a product space for representing the full Hamiltonian. This Hamiltonian contains additional small electrostatic terms connecting the core electrons with the promoted electron residing on the ligand system. It is these terms that produce the final splittings into states for each  $d\pi^*$  configuration. The type of coupling proposed here and the concept of ion parents are frequently employed to analyze complex atomic spectra. In this context the subject is discussed by Herzberg<sup>7</sup> and by Condon and Shortley.<sup>8</sup>